Ternary Blend Hybrid Solar Cells Incorporating Wide and Narrow Bandgap Polymers

Hyung Do Kim,[†] Hideo Ohkita,*[,†,‡] Hiroaki Benten,[†] and Shinzaburo Ito[†]

[†]Department of Polymer Chemistry, Graduate School of Engineering, Kyoto University, Katsura, Nishikyo, Kyoto 615-8510, Japan
[‡]Japan Science and Technology Agency (JST), PRESTO, 4-1-8 Honcho, Kawaguchi, Saitama 332-0012, Japan

S *Supporting Information*

ABSTRACT: Ternary hybrid solar cells based on zinc oxide with wide bandgap poly(3-hexylthiophene) (P3HT) and narrow bandgap poly[2,3-bis(3-octyloxyphenyl)quinoxaline-5,8-diyl-*alt*-thiophene-2,5-diyl] (PTQ1) exhibit improved photovoltaic performance compared to that of individual binary hybrid solar cells. The increase in the photocurrent is partly due to the complementary absorption bands, which can extend the light-harvesting range from visible to near-infrared regions, and partly due to efficient energy transfer from P3HT to PTQ1, by which P3HT excitons are more efficiently collected at the PTQ1/ZnO interface and hence convert to charge carriers effectively. Furthermore, the improvement in the fill factor may be due to efficient hole transfer from PTQ1 to P3HT with higher hole mobility, and thereby, hole polarons are more efficiently collected on the electrode.

KEYWORDS: ternary hybrid solar cells, narrow bandgap polymer, low bandgap polymer, ZnO, precursor, energy transfer, hole transfer
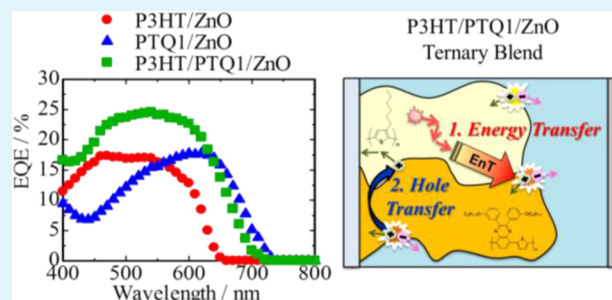
INTRODUCTION

Hybrid solar cells based on blends of a conjugated polymer and an inorganic material have attracted a great deal of attention because they can integrate both advantages of organic and inorganic materials.[1,2] In particular, ZnO has several advantages of high electron mobility and dielectric constant, being nontoxic and inexpensive, and its easy synthesis via a variety of techniques[3,4] and therefore has been applied to hybrid solar cells as an electron-transporting material. However, device performance still remains at ~2%,[1–4] which is much lower than that of organic solar cells. This is partly due to the incompatibility of organic and inorganic materials and partly due to the low light-harvesting efficiency of inorganic materials. To overcome these limitations, we have recently reported dye sensitization of hybrid solar cells fabricated from a blend solution of poly(3-hexylthiophene) (P3HT), a diethyl zinc precursor to ZnO, and a near-infrared (near-IR) dye.[5] Interestingly, most dye molecules are spontaneously segregated at the interface of P3HT and ZnO and hence can enhance the light-harvesting efficiency.[5] This is probably because of the crystallization of P3HT and the intermediate surface energy of dye molecules between P3HT and ZnO. Furthermore, a recent spectroscopic study has shown that such interfacial dye loading can accomplish both efficient charge separation and reduced charge recombination at the P3HT/ZnO interface.[6] However, dye sensitization is still not sufficient to harvest a wider range of solar light because of the sharp and narrow absorption band of dye molecules. Ternary blends based on two donor polymers and fullerene have been reported to widen the light-harvesting region because of complementary absorption bands ranging from the visible to

near-IR region.[7–15] Interestingly, in some combinations of materials, the open-circuit voltage (V_{OC}) varies linearly with the blend composition of mixed donor polymers, which is explained by the parallel-linkage model[7,8] or the donor alloy model.[9,10] However, there have few reports of the successful creation of ternary blend hybrid solar cells.

Herein, we report ternary hybrid solar cells based on blends of ZnO, wide bandgap poly(3-hexylthiophene) [P3HT (Figure 1a)], and narrow bandgap poly[2,3-bis(3-octyloxyphenyl)-quinoxaline-5,8-diyl-*alt*-thiophene-2,5-diyl] [PTQ1 (Figure 1a)]. As shown in Figure 1b, P3HT and PTQ1 have complementary broad absorption bands in the visible and near-IR region, respectively, and therefore are suitable materials for the collection of many more photons from solar light. Furthermore, as shown in Figure 1a, there are energy offsets in the levels of both the highest occupied molecular orbitals (HOMO) and the lowest unoccupied molecular orbitals (LUMO) that are enough to cause efficient charge transfer at the heterojunction of P3HT/ZnO and PTQ1/ZnO. Therefore, both polymers can serve as donors to ZnO in ternary hybrid solar cells. Figure 1c shows the schematic illustration of a layered structure in hybrid solar cells (ITO|PEDOT:PSS|P3HT/PTQ1/ZnO|Al).
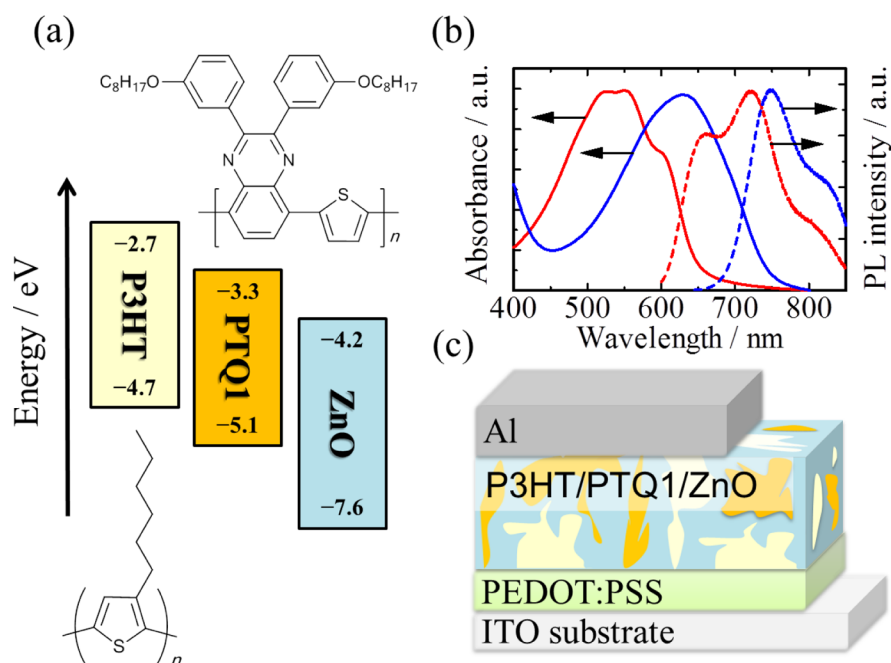
Figure 1. (a) Energy diagrams of the materials employed in this study and chemical structures of P3HT and PTQ1. (b) Absorption (—) and photoluminescence (---) spectra of P3HT (red) and PTQ1 (blue) neat films. (c) Schematic illustration of the device structure of P3HT/PTQ1/ZnO ternary hybrid solar cells.

RESULTS AND DISCUSSION

Figure 2 shows the absorption spectra of P3HT/PTQ1/ZnO ternary blend films. As shown in the figure, ternary blend films
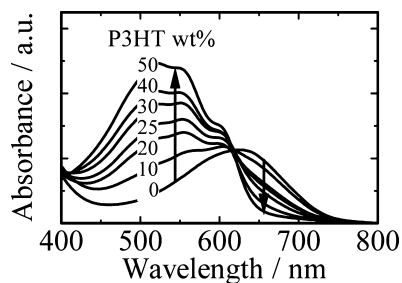

Figure 2. Absorption spectra of P3HT/PTQ1/ZnO ternary blends with various weight fractions of two polymers (x:50 − x:50 [P3HT]:[PTQ1]:[ZnO]).

exhibit wide absorption bands in the wavelength region from 400 to 750 nm because of a linear combination of the two absorption bands of wide bandgap P3HT and narrow bandgap PTQ1. Interestingly, vibronic bands were observed at 518, 558, and 608 nm, which are attributed to the 0−2, 0−1, and 0−0 transitions[16,17] of P3HT crystalline films,[18,19] respectively. This finding suggests that the crystallization of P3HT is not hindered even in the ternary blend films.

Figure 3 shows the atomic force microscopy (AFM) height images of binary and ternary blend films. As shown in the figure, all the blend films exhibited aggregated structures of small spherical grains that were tens of nanometers in diameter, which is consistent with previous reports.[20−22] These spherical grains may be already formed in solution prior to spin-coating, and the remaining polymer chains in solution adhere to the surface of the spherical structures during the spin-coating as reported previously.[21] Considering inefficient photoluminescence (PL) quenching efficiency (∼50%) of individual binary blend films (see the Supporting Information), we ascribe these grains to
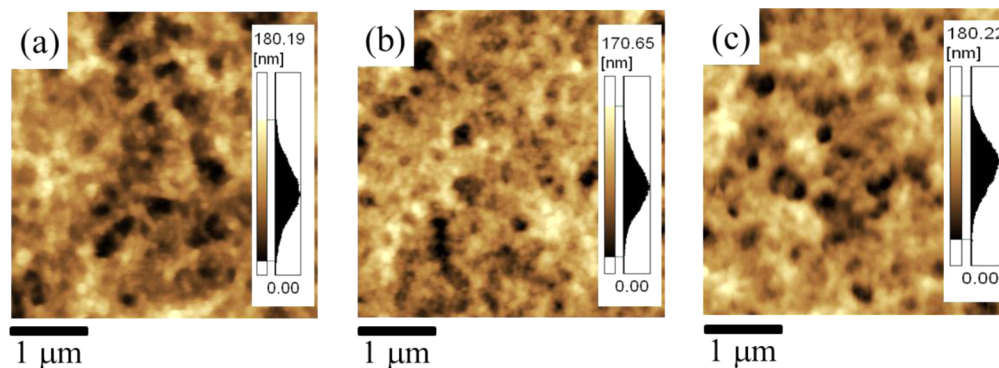

Figure 3. AFM height images (4 μm × 4 μm) of binary and ternary blend films: (a) P3HT/ZnO [5:5 (w/w)] binary blend film (rms of 35 nm), (b) PTQ1/ZnO [5:5 (w/w)] binary blend film (rms of 30 nm), and (c) P3HT/PTQ1/ZnO [3:2:5 (w/w)] ternary blend film (rms of 33 nm).

ZnO nanoparticles containing small amounts of donor polymers. In either case, the blend morphology was similar regardless of the blend composition, which is in good agreement with that found in the SEM images (see the Supporting Information). We therefore conclude that there is no distinct difference in the morphology on a scale of micrometers between binary and ternary blend films.

Figure 4 shows the $J-V$ characteristics of P3HT/PTQ1/ZnO [3:2:5 (w/w)] ternary hybrid solar cells and P3HT/ZnO [5:5

Figure 4. $J-V$ characteristics of P3HT/PTQ1/ZnO ternary hybrid solar cells and binary control subcells: P3HT/ZnO [5:5 (w/w)] binary hybrid solar cell (●), PTQ1/ZnO [5:5 (w/w)] binary hybrid solar cell (▲), and P3HT/PTQ1/ZnO [3:2:5 (w/w)] ternary hybrid solar cell (□).
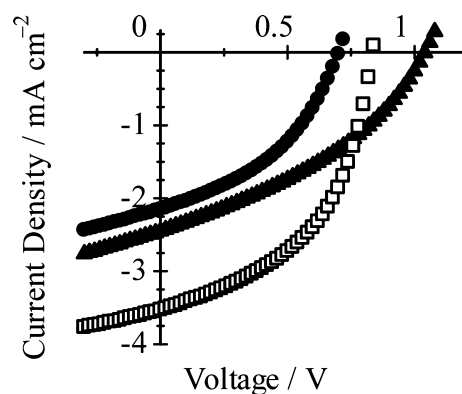
(w/w)] and PTQ1/ZnO [5:5 (w/w)] binary hybrid solar cells under AM1.5G illumination with an intensity of 100 mW cm^{-2}. The ternary hybrid cell exhibited a larger short-circuit current density (J_{SC}) and fill factor (FF) and an intermediate open-circuit voltage (V_{OC}) and hence improved power conversion efficiency (PCE) compared to those of the individual binary hybrid cells. As summarized in Figure 5, J_{SC} and FF of these devices showed maxima at 20 wt % PTQ1. On the other hand, V_{OC} increased from 0.70 V (P3HT/ZnO) to 1.04 V (PTQ1/ZnO) with an increasing PTQ1 fraction. As a result, the overall PCE was optimized at 20 wt % PTQ1: J_{SC} = 3.53 mA cm^{-2}, V_{OC} = 0.84 V, FF = 0.50, and PCE = 1.5%. This is larger by factors of 2.3 and 1.6 than those of P3HT/ZnO and PTQ1/ZnO binary hybrid solar cells, respectively.

We next measured the external quantum efficiency (EQE) spectra of the optimized ternary hybrid solar cell and the individual binary solar cells to address the origin of the increase in J_{SC}. As shown in Figure 6, the ternary hybrid solar cell exhibited an EQE over the broad wavelength region from 400 to 750 nm higher than that of the binary control solar cells. This is due to the complementary broad absorption bands of P3HT and PTQ1 as mentioned above. More interestingly, the EQE of the optimized ternary device is much higher than that predicted from the sum of the EQE of P3HT/ZnO and PTQ1/ZnO binary devices considering the weight fraction. As mentioned above, there is no distinct difference in the morphology of the blends. Thus, this improvement in the EQE suggests additional charge generation mechanisms. First, the improved EQE at the P3HT band (400−600 nm) is most probably due to the energy transfer from P3HT to PTQ1. Second, the improved EQE at the PTQ1 band (600−700 nm) can be ascribed to the hole transfer from PTQ1 to P3HT with higher mobility in ternary blend films, which would provide an additional charge transport channel and hence improve photocurrent generation. Such hole transfer is
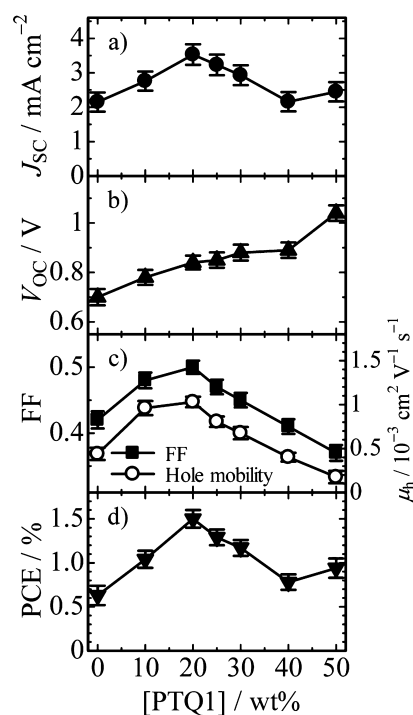

Figure 5. Device parameters of these solar cells plotted against PTQ1 weight fraction: a) J_{SC}, b) V_{OC}, c) FF (left axis) and hole mobility (right axis), and d) PCE. All the photovoltaic parameters were averaged for at least 10 devices.
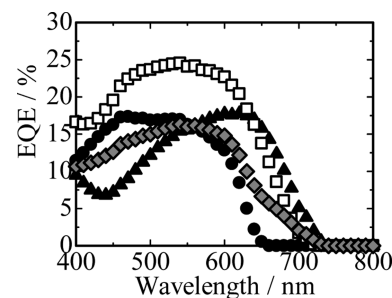

Figure 6. EQE spectra of P3HT/PTQ1/ZnO ternary hybrid solar cells and binary control subcells: P3HT/ZnO [5:5 (w/w)] binary hybrid solar cell (●), PTQ1/ZnO [5:5 (w/w)] binary hybrid solar cell (▲), P3HT/PTQ1/ZnO [3:2:5 (w/w)] ternary hybrid solar cell (□), and a theoretically predicted one from the sum of the EQE of each binary subcell considering the weight fraction of two donor polymers (gray diamonds).

consistent with efficient PL quenching of PTQ1 in P3HT/PTQ1/ZnO ternary blends compared to that in PTQ1/ZnO binary blends (see the Supporting Information). This charge transfer can be generally involved in ternary organic solar cells[7,8,11−13] and is supported by spectroscopic studies.[11,13]

To validate the transfer of energy from P3HT to PTQ1, we have measured the PL quenching of P3HT/PTQ1 binary blends upon the excitation of P3HT at 540 nm (see the Supporting Information). As shown in Figure S2 of the Supporting Information, the PL of PTQ1 was smaller than that from a PTQ1 neat film with the same absorbance, which probably contributed to the efficient charge transfer at the interface of P3HT and PTQ1. In particular, as shown in Figure S3 of the Supporting Information, the quenching efficiency of P3HT to PTQ1 increased more rapidly than that of PTQ1 to P3HT with

an increasing fraction of the other donor polymer in ternary blends. This finding implies that there is another quenching mechanism for P3HT excitons. Most probably, P3HT excitons are more efficiently quenched by the transfer of energy to PTQ1 because of the large spectral overlap between the P3HT emission and PTQ1 absorption bands. On the basis of these spectra, the Förster radius for the energy transfer is estimated to be 3.0 nm (see the Supporting Information), suggesting that more P3HT excitons generated even far from the interface can be transferred to PTQ1 domains intermixed with ZnO and thus effectively contribute to photocurrent generation. Such efficient exciton harvesting from P3HT to the third component (dye or polymer) in ternary blend solar cells has been reported by several groups, including ours.[5,15,23−25]

Next, we focus on the variation in V_{OC} of ternary hybrid solar cells. As shown in Figure 5b, V_{OC} of P3HT/PTQ1/ZnO ternary cells gradually increased from 0.70 V at 0 wt % PTQ1 to 0.89 V at 40 wt % PTQ1 and then jumped to 1.04 V at 50 wt %. This stepwise increase in V_{OC} suggests that the recombination sites are attributed mainly to P3HT/ZnO and partly to PTQ1/ZnO in this ternary blend. This is probably because of hole transfer from PTQ1 to P3HT as mentioned above. In other words, as shown in Figure 7, hole polarons are transported mainly in P3HT domains
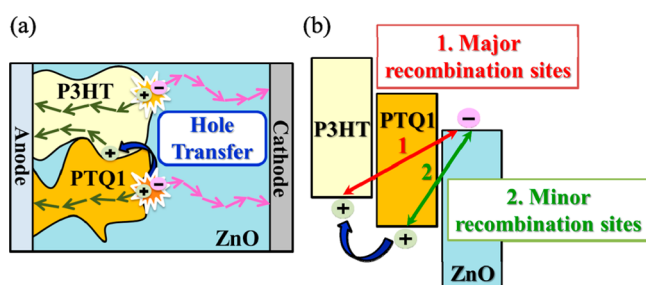

Figure 7. Schematic illustration of P3HT/PTQ1/ZnO ternary hybrid solar cells: (a) ternary blend structure and (b) energetic diagram of these devices.

and partly in PTQ1 domains in ternary hybrid solar cells. This would be beneficial for efficient hole transport in ternary hybrid solar cells because of the higher hole mobility of P3HT.

Finally, we discuss the dependence of FF as shown in Figure 5c on the basis of the hole carrier mobility (μ_h) in P3HT/PTQ1/ZnO ternary blend films with various blend ratios measured by the space-charge-limited current (SCLC) technique[26,27] (see the Supporting Information). As shown in Figure 5c, the hole mobility (μ_h) of P3HT/PTQ1/ZnO ternary devices increased from 4.4×10^{-4} cm^2 V^{-1} s^{-1} at 0 wt % PTQ1 (P3HT/ZnO), reached a maximum of 1.0×10^{-3} cm^2 V^{-1} s^{-1} at 20 wt % PTQ1, and then decreased to 1.8×10^{-4} cm^2 V^{-1} s^{-1} at 50 wt % PTQ1 (PTQ1/ZnO). This tendency is in good agreement with the dependence of FF. The improved FF in P3HT/PTQ1/ZnO ternary solar cells may be explained by the increased hole carrier mobility in the optimized ternary blends. The improvement in hole carrier mobility (μ_h) may be due to more appropriate phase separation than in the binary blends as reported previously.[28] Further studies are required for an in-depth understanding of the role of morphology in ternary hybrid solar cells.

CONCLUSIONS

In summary, we have demonstrated ternary hybrid solar cells based on ZnO, wide bandgap P3HT, and narrow bandgap PTQ1 that have complementary broad absorption bands in the visible

and near-IR region. Device performance was optimized at a P3HT:PTQ1 polymer blend ratio of 30:20. In P3HT/PTQ1/ZnO ternary blends, P3HT excitons are efficiently transferred to PTQ1 domains by energy transfer and subsequently followed by efficient electron transfer to ZnO. On the other hand, PTQ1 excitons are efficiently quenched not only by electron transfer to ZnO but also by hole transfer to P3HT. Both additional quenching pathways result in photocurrent generation that is improved compared to that of binary control cells. Because of the hole transfer from PTQ1 to P3HT, hole polarons are mainly transported in P3HT domains with a higher hole mobility and partly in PTQ1 domains in P3HT/PTQ1/ZnO ternary hybrid solar cells. This is consistent with the stepwise increase in V_{OC} with increasing PTQ1 fractions in P3HT/PTQ1/ZnO ternary hybrid solar cells. The optimized ternary device exhibits the maximal FF, which probably originates from a hole mobility higher than that in each polymer film. As such, we conclude that ternary hybrid solar cells provide a simple and attractive strategy for extending the light-harvesting range not only in the visible region but also in the near-IR region.

EXPERIMENTAL SECTION

Materials. Poly(3-hexylthiophene) (P3HT; M_w = 87000 g mol^{-1}; regioregularity of >90%) and poly[2,3-bis(3-octyloxyphenyl)-quinoxaline-5,8-diyl-*alt*-thiophene-2,5-diyl] (PTQ1; M_w = 113000 g mol^{-1}; M_w/M_n = 2.4) were purchased from Aldrich and Solarmer Materials, Inc., respectively, and used without further purification. A diethylzinc solution (1.1 M solution in toluene) was also purchased from Aldrich and used after being diluted with tetrahydrofuran (THF) to reduce its reactivity.

Device Fabrication. A hole-transporting buffer layer (40 nm) of poly(3,4-ethylenedioxythiophene) with poly(4-styrenesulfonate) (PEDOT:PSS, H. C. Starck Clevios PH500) was prepared atop a UV−ozone-cleaned ITO-coated glass substrate (sheet resistance of 10 Ω per square) by spin-coating at 3000 rpm for 99 s and then heated on a hot plate at 140 °C for 10 min. The photoactive layer was prepared on the ITO/PEDOT:PSS substrate by spin-coating from a blend solution at 1200 rpm for 60 s in the nitrogen atmosphere under a relative humidity of 40%. The blend solutions, varying from weight fraction of two polymers, were obtained by mixing 0.70 mL of P3HT (x mg) and PTQ1 ($5 − x$ mg) in chlorobenzene with 0.30 mL of a 0.4 M diethylzinc solution, which was prepared by mixing 1.8 mL of a 1.1 M diethylzinc solution in toluene with 3.2 mL of tetrahydrofuran (THF). The mixed solution was stirred at 40 °C overnight. The active layers were aged for 15 min and then annealed on a hot plate at 140 °C for 15 min under the same condition described above. Assuming complete conversion of the diethylzinc to ZnO, the weight ratio of blend films is estimated to be x:50 − x:50 for a P3HT/PTQ1/ZnO ternary blend. The thickness of active layers varied from 80 to 95 nm according to the weight fraction of two polymers. After being heated, the samples were transferred to a glovebox under an inert nitrogen atmosphere. The Al electrode (100 nm) was thermally deposited on top of the active layer under high vacuum (<2.5 × 10^{-4} Pa). At least 10 devices were fabricated to ensure the reproducibility of the $J−V$ characteristics.

Measurements. UV−visible absorption and PL spectra were measured with a UV−visible−near-IR spectrophotometer (Hitachi, U-3500) and a fluorescence spectrophotometer (Horiba Jobin Yvon, FluoroLog-3) equipped with an iHR320 imaging detector, respectively. The $J−V$ characteristics were measured with a DC voltage and current source/monitor (Advantest, R6243) in the dark and under the illumination filtered by a UV filter with AM1.5G-simulated solar light with 100 mW cm^{-2}. The light intensity was corrected with a calibrated silicon photodiode reference cell (Peccell, PECSI01). The EQE spectra were measured with a digital electrometer (Advantest, R8252) under monochromatic light illumination from a 500 W xenon lamp (Thermo Oriel, 66921) with optical cutoff filters and a monochromator (Thermo Oriel, UV−visible Cornerstone). The active area of the device was 0.07

cm^2, and illumination was conducted from the ITO side. All these measurements were performed under a nitrogen atmosphere at room temperature. The film surface morphology and the film thickness were measured with an atomic force microscope (Shimadzu, SPM-9600) with a silicon probe (Olympus, a force constant of ~0.15 N m^{-1}) in contact mode. The SEM images were measured with a scanning electron microscope (Keyence, VE-9800) at an accelerating voltage of 2 kV.

■ ASSOCIATED CONTENT

ⓢ Supporting Information

PL quenching, SEM images, estimation of the Förster radius, and mobility measurements. This material is available free of charge via the Internet at http://pubs.acs.org.

■ AUTHOR INFORMATION

Corresponding Author

*Telephone: +81 75 383 2614. Fax: +81 75 383 2617. E-mail: ohkita@photo.polym.kyoto-u.ac.jp.

Notes

The authors declare no competing financial interest.

■ ACKNOWLEDGMENTS

■ REFERENCES

(1) Gao, F.; Ren, S.; Wang, J. The Renaissance of Hybrid Solar Cells: Progresses, Challenges, and Perspectives. *Energy Environ. Sci.* **2013**, *6*, 2020−2040.

(2) Li, S.-S.; Chen, C.-W. Polymer-Metal-Oxide Hybrid Solar Cells. *J. Mater. Chem. A* **2013**, *1*, 10574−10591.

(3) Moulé, A. J.; Chang, L.; Thambidurai, C.; Vidu, R.; Stroeve, P. Hybrid Solar Cells: Basic Principles and the Role of Ligands. *J. Mater. Chem.* **2012**, *22*, 2351−2368.

(4) Wright, M.; Uddin, A. Organic−Inorganic Hybrid Solar Cells: A Comparative Review. *Sol. Energy Mater. Sol. Cells* **2012**, *107*, 87−111.

(5) Kim, H. D.; Ohkita, H.; Benten, H.; Ito, S. Dye Sensitization in Polymer/ZnO/Dye Ternary Hybrid Solar Cells. *Chem. Lett.* **2013**, *42*, 825−827.

(6) Shen, Q.; Ogomi, Y.; Das, S. K.; Pandey, S. S.; Yoshino, K.; Katayama, K.; Momose, H.; Toyoda, T.; Hayase, S. Huge Suppression of Charge Recombination in P3HT−ZnO Organic−Inorganic Hybrid Solar Cells by Locating Dyes at the ZnO/P3HT Interfaces. *Phys. Chem. Chem. Phys.* **2013**, *15*, 14370−14376.

(7) Yang, L.; Zhou, H.; Price, S. C.; You, W. Parallel-like Bulk Heterojunction Polymer Solar Cells. *J. Am. Chem. Soc.* **2012**, *134*, 5432−5435.

(8) Yang, L.; Yan, L.; You, W. Organic Solar Cells beyond One Pair of Donor−Acceptor: Ternary Blends and More. *J. Phys. Chem. Lett.* **2013**, *4*, 1802−1810.

(9) Khlyabich, P. P.; Burkhart, B.; Thompson, B. C. Compositional Dependence of the Open-Circuit Voltage in Ternary Blend Bulk Heterojunction Solar Cells Based on Two Donor Polymers. *J. Am. Chem. Soc.* **2012**, *134*, 9074−9077.

(10) Street, R. A.; Davies, D.; Khlyabich, P. P.; Burkhart, B.; Thompson, B. C. Origin of the Tunable Open-Circuit Voltage in Ternary Blend Bulk Heterojunction Organic Solar Cells. *J. Am. Chem. Soc.* **2013**, *135*, 986−989.

(11) Koppe, M.; Egelhaaf, H. J.; Dennler, G.; Scharber, M. C.; Brabec, C. J.; Schilinsky, P.; Hoth, C. N. Near IR Sensitization of Organic Bulk Heterojunction Solar Cells: Towards Optimization of the Spectral Response of Organic Solar Cells. *Adv. Funct. Mater.* **2010**, *20*, 338−346.

(12) Ameri, T.; Min, J.; Li, N.; Machui, F.; Baran, D.; Forster, M.; Schottler, K. J.; Dolfen, D.; Scherf, U.; Brabec, C. J. Performance Enhancement of the P3HT/PCBM Solar Cells through NIR Sensitization Using a Small-Bandgap Polymer. *Adv. Energy Mater.* **2012**, *2*, 1198−1202.

(13) Koppe, M.; Egelhaaf, H. J.; Clodic, E.; Morana, M.; Lüer, L.; Troeger, A.; Sgobba, V.; Guldi, D. M.; Ameri, T.; Brabec, C. J. Charge Carrier Dynamics in a Ternary Bulk Heterojunction System Consisting of P3HT, Fullerene, and a Low Bandgap Polymer. *Adv. Energy Mater.* **2013**, *3*, 949−958.

(14) Ameri, T.; Heumüller, T.; Min, J.; Li, N.; Matt, G.; Scherf, U.; Brabec, C. J. IR Sensitization of an Indene-C60 Bisadduct (ICBA) in Ternary Organic Solar Cells. *Energy Environ. Sci.* **2013**, *6*, 1796−1801.

(15) Yan, H.; Li, D.; Zhang, Y.; Yang, Y.; Wei, Z. Rational Design of Ternary-Phase Polymer Solar Cells by Controlling Polymer Phase Separation. *J. Phys. Chem. C* **2014**, *118*, 10552−10559.

(16) Spano, F. C. Modeling Disorder in Polymer Aggregates: The Optical Spectroscopy of Regioregular Poly(3-hexylthiophene) Thin Films. *J. Chem. Phys.* **2005**, *122*, 234701−234715.

(17) Clark, J.; Silva, C.; Friend, R. H.; Spano, F. C. Role of Intermolecular Coupling in the Photophysics of Disordered Organic Semiconductors: Aggregate Emission in Regioregular Polythiophene. *Phys. Rev. Lett.* **2007**, *98*, 206406−206409.

(18) Erb, T.; Zhokhavets, U.; Gobsch, G.; Raleva, S.; Stühn, B.; Schilinsky, P.; Waldauf, C.; Brabec, C. J. Correlation Between Structural and Optical Properties of Composite Polymer/Fullerene Films for Organic Solar Cells. *Adv. Funct. Mater.* **2005**, *15*, 1193−1196.

(19) Ma, W.; Yang, C.; Gong, X.; Lee, K.; Heeger, A. J. Thermally Stable, Efficient Polymer Solar Cells with Nanoscale Control of the Interpenetrating Network Morphology. *Adv. Funct. Mater.* **2005**, *15*, 1617−1622.

(20) Beek, W. J. E.; Slooff, L. H.; Wienk, M. M.; Kroon, J. M.; Janssen, R. A. J. Hybrid Solar Cells Using a Zinc Oxide Precursor and a Conjugated Polymer. *Adv. Funct. Mater.* **2005**, *15*, 1703−1707.

(21) Beek, W. J. E.; Wienk, M. M.; Kemerink, M.; Yang, X.; Janssen, R. A. J. Hybrid Zinc Oxide Conjugated Polymer Bulk Heterojunction Solar Cells. *J. Phys. Chem. B* **2005**, *109*, 9505−9516.

(22) Oosterhout, S. D.; Koster, L. J. A.; van Bavel, S. S.; Loos, J.; Stenzel, O.; Thiedmann, R.; Schmidt, V.; Campo, B.; Cleij, T. J.; Lutzen, L.; Vanderzande, D.; Wienk, M. M.; Janssen, R. A. J. Controlling the Morphology and Efficiency of Hybrid ZnO:Polythiophene Solar Cells Via Side Chain Functionalization. *Adv. Energy Mater.* **2011**, *1*, 90−96.

(23) Honda, S.; Nogami, T.; Ohkita, H.; Benten, H.; Ito, S. Improvement of the Light-Harvesting Efficiency in Polymer/Fullerene Bulk Heterojunction Solar Cells by Interfacial Dye Modification. *ACS Appl. Mater. Interfaces* **2009**, *1*, 804−810.

(24) Honda, S.; Ohkita, H.; Benten, H.; Ito, S. Selective Dye Loading at the Heterojunction in Polymer/Fullerene Solar Cells. *Adv. Energy Mater.* **2011**, *1*, 588−598.

(25) Honda, S.; Yokoya, S.; Ohkita, H.; Benten, H.; Ito, S. Light-Harvesting Mechanism in Polymer/Fullerene/Dye Ternary Blends Studied by Transient Absorption Spectroscopy. *J. Phys. Chem. C* **2011**, *115*, 11306−11317.

(26) Lampert, M. A.; Mark, P. *Current Injection in Solids*; Academic Press: New York, 1970.

(27) Shen, Y.; Hosseini, A. R.; Wong, M. H.; Malliaras, G. G. How To Make Ohmic Contacts to Organic Semiconductors. *ChemPhysChem* **2004**, *5*, 16−25.

(28) Lu, K.; Fang, J.; Zhu, X.; Yan, H.; Li, D.; Di, C.; Yang, Y.; Wei, Z. A Facile Strategy to Enhance the Fill Factor of Ternary Blend Solar Cells by Increasing Charge Carrier Mobility. *New J. Chem.* **2013**, *37*, 1728−1735.